# Comparative study of EVA-Cloisite® 20A and heat-treated EVA-Cloisite® 20A on heavy-metal adsorption properties

**Derrick S Dlamini, Ajay K Mishra* and Bhekie B Mamba**
*Department of Applied Chemistry, University of Johannesburg, PO Box 17011, Doornfontein 2028, Johannesburg, South Africa*

## Abstract

Ethylene vinyl acetate (EVA)/ **Cloisite® 20A** (C20A) composite fabricated via the melt-blending method was used for the development of a heavy-metal adsorbent through acid and heat treatment. Heat-treated composites were produced at 400°C to 1 000°C in air and $N_2$ atmospheres. The materials were characterised through TGA, FT-IR, contact angle and Zetasizer. Treating EVA/C20A composites with $H_2SO_4$ at 130°C reduced the contact angle from 99.73° to 30.40°. The acid-functionalised composite was tested for the removal of $Pb^{2+}$ and an adsorption capacity of 49 mg·g$^{-1}$ was recorded while the heat-treated composite exhibited an adsorption capacity of 153 mg·g$^{-1}$.

**Keywords***:* ash, EVA, bentonite, activation, adsorption

## Introduction

Heavy-metal pollution is known to cause instability, disorder, harm or discomfort to living organisms (Al-Attar, 2011). Several studies have shown that heavy metals such as lead, zinc, cadmium, chromium and copper can be very toxic even at low concentrations (Periasamy and Namasivayam, 1996). Industrial and agricultural activities are a major source of heavy-metal pollution worldwide. In South Africa, for instance, industrial, mining and agricultural activities are considered as the driving force of the country's economy. Due to the rapid development of agriculture, industrial and traffic activities large amounts of heavy-metal pollutants are discharged to the local environment (Bai et al., 2011; Liua et al., 2011. The aggressive development of agriculture and industrial sectors makes it difficult to combat heavy-metal pollution. It has been reported that landfill is the best available technology especially for developing countries for the disposal of solid waste; however, heavy-metal pollution by landfill leachate is still possible (Longa et al., 2011). Heavy metals may also end up in sewage effluents (Bystrzejewski et al., 2011).

Removal of heavy-metal ions from sewage effluents and other water resources is essential to ensure environmental and human safety. Several techniques like reverse osmosis, nanofiltration, ion exchange and adsorption have been used in the removal of heavy metals from water. The use of activated carbon (AC) as an adsorbent is a simple and economically viable method of pollutant removal (Vargas et al., 2011). According to Tongpoothorn et al. (2011) activated carbon is a widely-used adsorbent because of its extremely high surface areas, micropore volumes, large adsorption capacities, fast adsorption kinetics, and relative ease of regeneration.

In this study, a heavy-metal adsorbent was derived from EVA/C20A composites that had been synthesised via the melt-blending method. The melt-blending method has been gaining significant attention in the fabrication of polymeric composites with improved mechanical properties, relative to those produced by alternative composite fabrication strategies (solution blending and *in situ* polymerisation). Polymer/clay composites have been the centre of research over the past decade because of their potentially large application area. To ensure environmental safety, the materials should be discarded safely after use. Experiments in our laboratory have shown that EVA/C20A composites synthesised via the melt-blending method are hydrophobic and non-biodegradable in garden soil and compost. Therefore, we have derived a heavy-metal adsorbent from the EVA/C20A composite through acid and heat treatments of the non-biodegradable composites. The treatment methods were compared. Both procedures were kept as simple as possible to minimise costs. Bench-scale experiments on the removal of $Pb^{2+}$ from aqueous solution were undertaken to test the potential application of the novel adsorbent in heavy-metal removal from water. Equilibrium and kinetic models were extensively applied on the adsorption results in order to establish whether the adsorbent is suitable for heavy-metal removal. The results indicate that composites used for different purposes may still be reused in adsorption technology after acid or heat treatment.

## Experimental

### Materials

Ethylene vinyl acetate (EVA) with 9% vinyl acetate (VA) was supplied by Plastamid, South Africa. The density of EVA was 0.930 g·cm$^{-3}$ and the melting point was 95°C. Cloisite® 20A (C20A), a natural montmorillonite clay modified with dimethyl dihydrogenated to allow quaternary ammonium salt – CEC = 95 meq·100 g$^{-1}$, was obtained from Southern Clay Products, Texas, USA. Concentrated acids (HCl and $H_2SO_4$) and KOH were sourced from Aldrich Chemicals, South Africa.

### Preparation of adsorbent

The EVA/C20A was fabricated and characterised for thermal and morphological properties as discussed in our work

* To whom all correspondence should be addressed.
☎ +27 11 559 6180; fax: +27 11 559 6425;
e-mail: amishra@uj.ac.za
*Received 5 December 2011; accepted in revised form 9 July 2012.*

http://dx.doi.org/10.4314/wsa.v38i4.6
Available on website http://www.wrc.org.za
ISSN 0378-4738 (Print) = Water SA Vol. 38 No. 4 July 2012
ISSN 1816-7950 (On-line) = Water SA Vol. 38 No. 4 July 2012

previously published (Dlamini et al., 2011a; b). The adsorbent was derived through acid and heat treatments. To prepare the acid-treated adsorbent, a composite strip was oxidised with concentrated $H_2SO_4$ at a ratio of 1:2 (weight) and heated at 130°C in an oven for 24 h. The dry curing was meant to catalyse the oxidation process. The acidified composite was allowed to cool and thereafter the free acid was removed by rinsing the composite material with deionised water until the filtrate reached a pH of between 6.5 and 7.5, after which it was then dried in an oven at 100°C for 24 h. Heat-treated composite adsorbents were derived from the EVA/C20A composite strip at different temperatures: 400°C, 500°C, 600°C, 700°C, 800°C, 900°C, and 1 000°C, for a period of 15 min in air and $N_2$ atmospheres.

### Characterisation of adsorbent

#### *Thermogravimetric analysis (TGA)*

Thermogravimetric analyses were performed to approximate the EVA residue after heating. The analyses were done in a Perkin Elmer TGA 4000 Analyzer equipped with Pyris™ Software. The sample mass was 8–10 mg and the temperature ranged from 100 ºC to 600ºC at a heating rate of 15°C·min$^{-1}$. The analyses were performed under nitrogen atmosphere at a flow rate of 15 mℓ·min$^{-1}$.

#### *Contact angle measurements*

The hydrophilic/hydrophobic nature of the composite strips, before and after acid treatment, was examined by using contact angle (CA) measurements using the sessile-drop method. The measurements were done on a Dataphysics Optical Contact Angle SCA20 at a dosing volume of 12 µℓ. The values are given from an average of 6 measurements made at different locations on the specimen surface.

### Zetasizer analysis

Zeta potential and particle size were investigated using a Zetasizer Nano ZS from Malvern Instruments. The dispersant was water with a pH of 5.5.

#### *ATR-FT-IR analysis*

The functional properties were measured directly by Bruker Tensor 27 FT-IR spectrometer and analysed with OPUS software. With this ATR-FT-IR model (attenuated total reflectance (ATR) Fourier transform infrared (FT-IR) model) the samples were analysed as they were. A small piece of sample was sliced from the polymeric composite material and was analysed. Prior to analysis, the samples were dried in an oven overnight.

### Batch adsorption studies

The batch experiment technique was adopted for bench-scale adsorption experiments to study the heavy-metal adsorption capabilities of the composites using $Pb^{2+}$ as an analyte. The experiments were carried out in 25 mℓ stopper reagent bottles. A stock solution of $Pb^{2+}$ solution (200 mg·ℓ$^{-1}$) was prepared by dissolving 0.319 g of lead nitrate salt in deionised water. Batch adsorption experiments were conducted to establish the optimum pH, contact time and adsorbent dose, and the effect of temperature and initial concentration on $Pb^{2+}$ adsorption. The adsorbent weight was 20 mg and the volume of the analyte solutions was 20 mℓ, unless otherwise specified. Initial pH of the solution was adjusted using 0.1M KOH or HCl. After adsorption the solutions were analysed for the remaining $Pb^{2+}$ concentration using atomic adsorption spectroscopy (AAS).

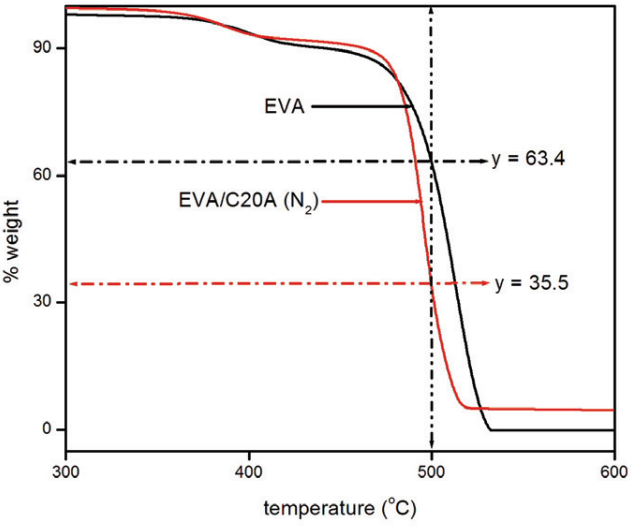


***Figure 1***
*TGA curves of neat EVA and the EVA/C20A heat-treated composites*

### Adsorption isotherms and kinetic models

Methods and supporting information used for the analysis of adsorption isotherms and kinetics are described in Appendix 1 (Langmuir, Freundlich, pseudo-first-order, pseudo-second-order, Natarajan and Khalaf, and Elovich models).

## Results and discussion

### TGA

The thermal degradation mechanism in char-forming polymers like EVA may be described as a generalised chemical bond scission process consisting of primary and secondary decomposition events (Bahramian et al., 2008). Generally, the degradation of EVA occurs via a 2-step mechanism with the loss of acetic acid during the first step (300°C to 400°C) and random chain scission of the remaining material in the second step, to form unsaturated vapour species (≈ 430ºC), such as butene and ethylene (Hull et al., 2003). The thermographs of the composite and neat EVA are shown in Fig. 1.

The catalytic effect of layered silicates on crosslinking/charring reactions derives mainly from the acid sites formed on silicates due to the degradation of the organic treatment of the clay (Kiliaris and Papaspyrides, 2010). The degradation of C20A is discussed in our previous work published on EVA/C20A composites (Dlamini et al., 2011a; b).

The percentage weight loss in each TGA curve clearly suggests that the clay residue after thermal degradation corresponds to the 5% clay dosage. Of most interest to this study was the residue at 500°C marked with the horizontal arrows in each TGA curve. It can be seen that about 35.5% (weight) EVA residue remains at 500°C. The EVA residue is essential in the sense that it suggests that we still have a composite.

### FT-IR analysis

The FT-IR results of the EVA/C20A composite and the functionalised EVA/C20A composite are shown in Fig. 2. The peaks located at 2 917 cm$^{-1}$ and 2 849 cm$^{-1}$ were attributed to ν(CH) and ν(CH2) groups, respectively, (Dlamini et al., 2011a) and


http://dx.doi.org/10.4314/wsa.v38i4.6
Available on website http://www.wrc.org.za
ISSN 0378-4738 (Print) = Water SA Vol. 38 No. 4 July 2012
ISSN 1816-7950 (On-line) = Water SA Vol. 38 No. 4 July 2012

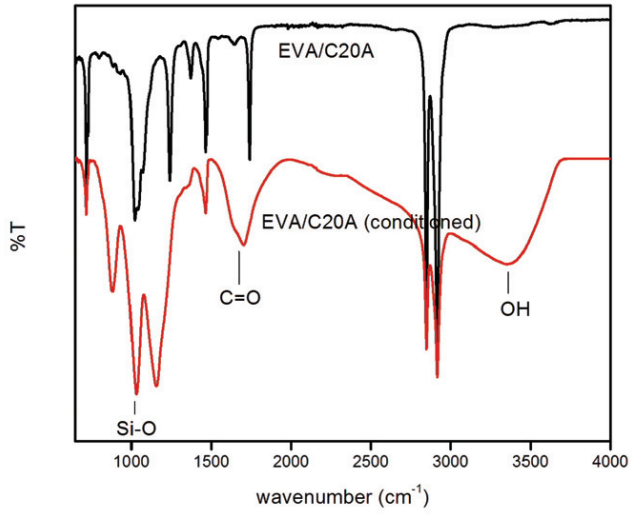


***Figure 2***
*FT-IR spectra: EVA/C20A and acid-treated EVA/C20A composites*

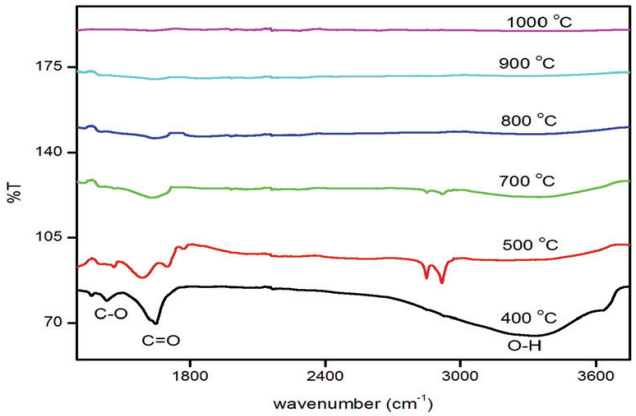


***Figure 3***
*FT-IR spectra of heat-treated composite*

the broad peak located at 3 351 $cm^{-1}$ was assigned to the ν(OH) group.

In the carbonyl region (1 600$^{-1}$ to 1 800 $cm^{-1}$) there is a peak at 1 704 $cm^{-1}$ attributed to ν(C=O). Noteworthy, the ν(C=O) peak in the un-functionalised composite is shifted about 35 $cm^{-1}$ higher indicating that the carbonyl bond is shorter in C=O, most likely because it belongs to the COOC component whereas in the oxidised composite it belongs to the COOH component, which may have resulted from the elimination of the acetate group in EVA. The band at 1 439 $cm^{-1}$ resulted from the C–O stretching of the carboxylate anion in carboxylic groups and the band at 1 654 $cm^{-1}$ was attributed to C=O stretching vibration modes in carbonyl groups (Han et al., 2011; Wang et al., 2011; Wei et al., 2011). The spectra show a broad and strong peak at 1 020 $cm^{-1}$ which was confidently assigned to Si-O adsorption.

The FT-IR results of the heat-treated composites are shown in Fig. 3. The heat-treated composites were obtained by heating the acid-functionalised composites at different temperatures ranging from 400°C to 1 000°C.

The results indicate that the heating at higher temperatures resulted in the degradadation of the functional groups introduced during the heat treatment.

## Contact angle

Contact angles provide useful information regarding surface hydrophilicity. The rate at which water wets the composite determines how easily the water can penetrate the composite assemblage. Mixing EVA with the clay increased the contact angle from 95.60° to 99.73° and the polar component consequently decreased from 19.18 $mJ{\cdot}m^{-2}$ to 10.31 $mJ{\cdot}m^{-2}$. This is understandable because both materials are hydrophobic. After oxidation, the contact angle of the composite substantially decreased from 99.73° to 30.40° with a polar component of 44.86 $mJ{\cdot}m^{-2}$. The reductions in the polar components suggest a decrease in the hydrophobic character (Bessadok et al., 2007).

## Zetasizer analysis

The zeta potential results are summarised in Table 1. For the heat-treated composites, the composites derived at 500°C were used.

**Table 1**
**Particle size and zeta potential**

| Material | Zeta potential | |
|---|---|---|
| | Air | $N_2$ |
| C20A | −38.7 | −40.5 |
| EVA | −25.7 | - |
| EVA/C20A | −33.1 | −37.6 |

Visual comparison of the composite produced under the different atmospheres showed that the composite derived in air was more like ash. The argument that the heat-treated composite was composed of EVA residue was justified by heating pure EVA as a reference experiment. Zeta potential results show that all the materials are negatively charged. The nucleophilic nature of the adsorbents suggests that the composites will interact chemically with $Pb^{2+}$.

## Heavy-metal adsorption

### *Effect of heating temperature*

The purpose of acid/heat treatment of the composites was to improve the surface area and provide physicochemical alterations in the structure of the clay. The effect of heating temperature (in air) on the modified composite and its adsorption capacity for $Pb^{2+}$ was investigated. The uptake of $Pb^{2+}$ was calculated by using the following equation:

$$R(\%) = 100 \times \frac{C_o - C_t}{C_o} \quad (1)$$

where:

$C_o$ and $C_t$ ($mg{\cdot}\ell^{-1}$) are the highest initial $Pb^{2+}$ concentration and remaining concentration at time ($t$), respectively.

The temperatures selected were 400°C, 500°C, 600°C, 700°C, 800°C, 900°C and 1 000°C. The results, given in Fig. 4, show a sharp increase from 400°C to 500°C and thereafter a substantial decrease from 500°C to 900°C in per cent $Pb^{2+}$ uptake.

Koyuncu (2008) activated bentonite at 600°C. In the present work, 500°C was found to be the optimum temperature for heat treatment of carbonised EVA/C20A composites for the adsorption of $Pb^{2+}$. This can be attributed to the destruction of the adsorption active sites (–COOH) as shown in FT-IR at temperatures higher than 500°C leaving only silica and alumina behind.

http://dx.doi.org/10.4314/wsa.v38i4.6
Available on website http://www.wrc.org.za
ISSN 0378-4738 (Print) = Water SA Vol. 38 No. 4 July 2012
ISSN 1816-7950 (On-line) = Water SA Vol. 38 No. 4 July 2012

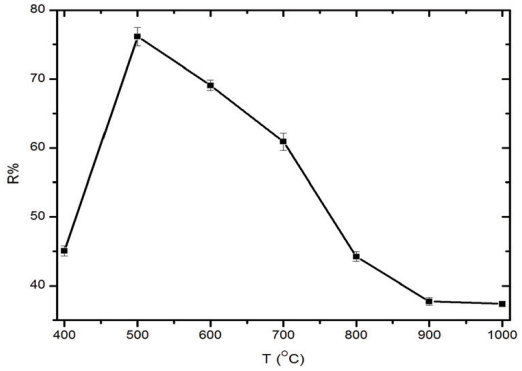


**Figure 4**
*Effect of heating temperature on the adsorption of $Pb^{2+}$ at an initial concentration of 200 mg·ℓ$^{-1}$ at pH 5.5*

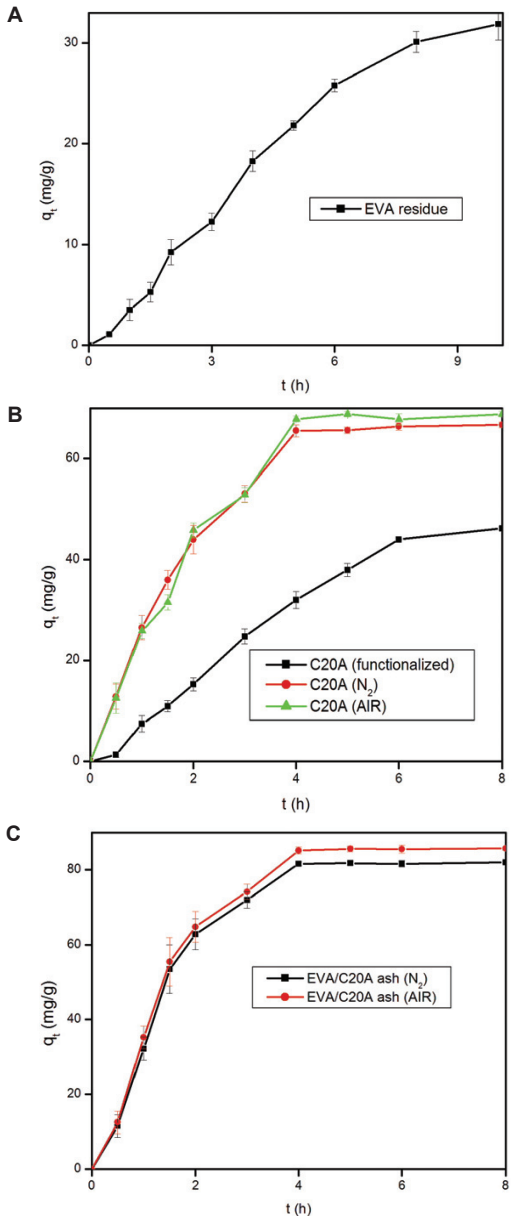


**Figure 5**
*Effect of heating atmosphere on the adsorption capacity of the adsorbents at pH 5.5 and initial concentration of 100 mg·ℓ$^{-1}$*
*A: EVA heated in air; B: C20A;*
*C: heat-treated EVA/C20A composites*

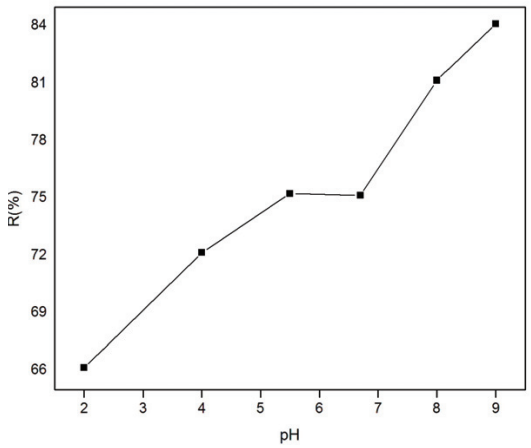


**Figure 6**
*Effect of pH on the adsorption of $Pb^{2+}$ by the heat-treated (in air) composite at an initial concentration of 200 mg·ℓ$^{-1}$ in 3 h*

### *Effect of heating atmosphere*

The atmospheres used were air and $N_2$. The results are shown in Fig. 5. The effect of heating atmosphere on the adsorption properties of the adsorbents was tested on EVA (Fig. 5A), C20A (Fig. 5B), and on the EVA/C20A composite (Fig. 5C). Under $N_2$ atmosphere, EVA formed a gel which solidified after cooling.

Apparently, there is little change in the adsorption properties of the adsorbent thermally treated in either air or $N_2$. The EVA residue had the lowest adsorption capacity, probably because of the absence of silicates. The results are consistent with the data obtained from Zetasizer analyses. Based on these results, the composite derived under air conditions was used forthwith for all adsorptions with heat-treated composites.

### *Effect of pH*

Optimisation of pH for sorption medium plays an important role in sorption studies (Hosseini-Bandegharaei et al., 2011). This is because the hydronium ions are strong competing adsorbate ions and partly due to the fact that the pH of a solution influences the chemical speciation of the metal ions in solution. The amount of $Pb^{2+}$ adsorbed to the heat-treated (in air) composite, expressed in terms of adsorption efficiency as a function of pH, is shown in Fig. 6.

The adsorption increased with increase in the pH of the solution until pH 5.5. The low uptakes at low pH were attributed to a competitive adsorption as a result of high concentrations of hydronium ions ($H_3O^+$) which compete for adsorption sites with $Pb^{2+}$. The observed adsorption increased with increasing pH and this was attributed to an increase in the concentration of $Pb(OH)^+$ resulting in the decline in the hydronium ion concentration. For pH values >7.0, a new increase in $Pb^{2+}$ uptake is observed as a result of the chemical precipitation of the metal in the form of hydroxide. Therefore, the $Pb^{2+}$ adsorption phenomenon in aqueous solution at 100 mg·ℓ$^{-1}$ occurs at pH below 6.0.

### Adsorption time profile: Acid vs. heat treatment

The adsorbents prepared by acid treatment were compared to the adsorbents prepared via heat treatment in terms of adsorption capacity ($q_t$). The sorption capacity is one of the most important parameters of the sorbent characteristics in the sense that it determines how much of the heavy-metal pollutant can


http://dx.doi.org/10.4314/wsa.v38i4.6
Available on website http://www.wrc.org.za
ISSN 0378-4738 (Print) = Water SA Vol. 38 No. 4 July 2012
ISSN 1816-7950 (On-line) = Water SA Vol. 38 No. 4 July 2012

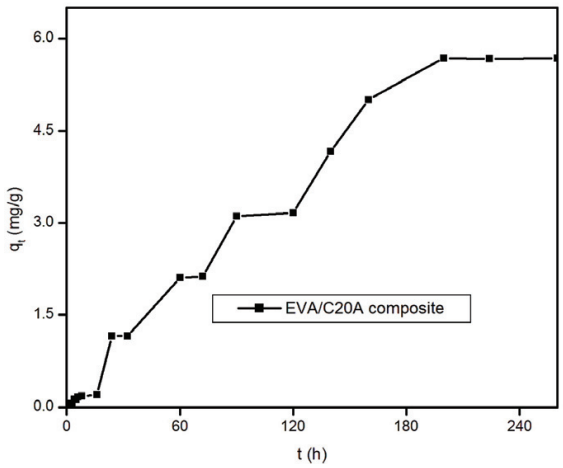


***Figure 7***
*Adsorption of $Pb^{2+}$ on EVA/C20A composite at an initial concentration of 100 mg·ℓ$^{-1}$ and pH 5.5*

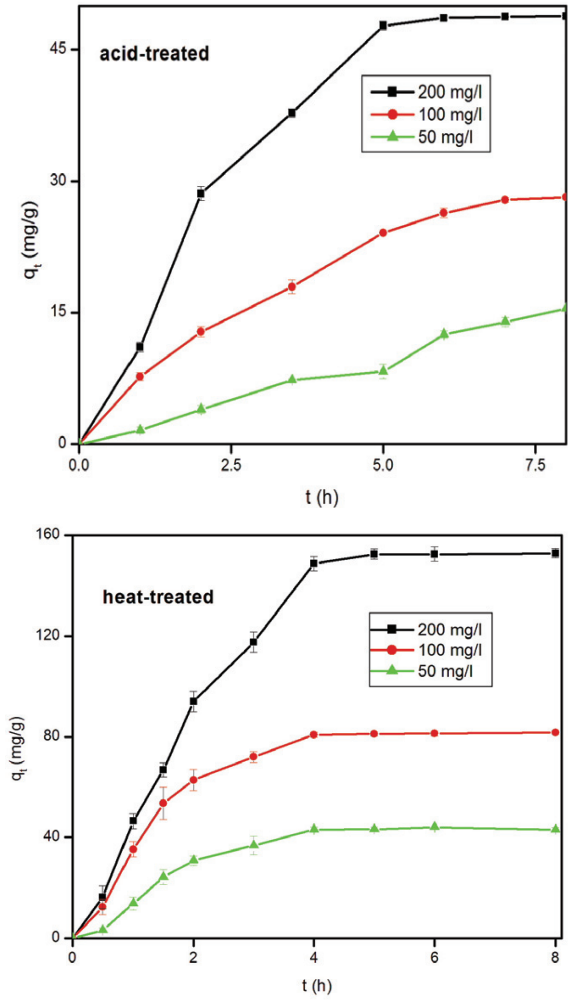


***Figure 8***
*Adsorption time profiles for the uptake of $Pb^{2+}$ at pH 5.5: Acid-treated vs. heat-treated (in air) composites*

be removed from the aqueous solution by a unit mass of the sorbent (Bystrzejewski et al., 2011). The adsorption capacity ($q_t$) was calculated using the following equation:

$$q_t = \frac{(C_o - C_t)v}{w_s} \quad (2)$$

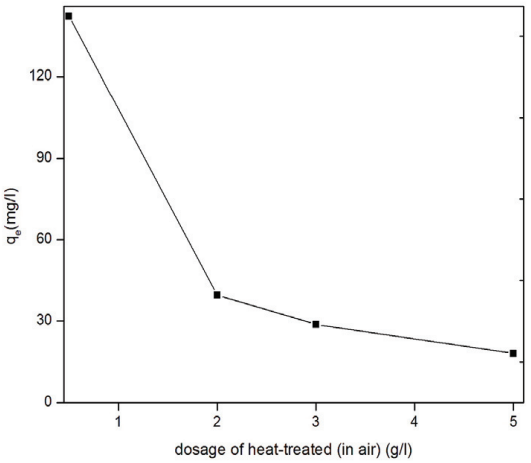


***Figure 9***
*Effect of dosage of adsorbent (composite heat-treated in air) at an initial concentration of 100 mg·ℓ$^{-1}$ and pH 5.5*

where:

$C_o$ and $C_t$ represent the initial concentration and the remaining concentration at different time intervals

$v$ is the volume of the solution

$w_s$ is the weight of the composite

Figure 7 depicts the adsorption capacity of untreated EVA/C20A composite. The plots given in Fig. 8 show the adsorption kinetics of $Pb^{2+}$ adsorbed onto the acid-treated (A) and heat-treated in air (B) composite. It can be seen that the adsorption of $Pb^{2+}$ on the composite increased steadily until equilibrium was attained, i.e, after about 6 h for acid-treated and 4 h for heat-treated composites, respectively. The maximum adsorption capacities were 153 mg·g$^{-1}$ for heat-treated and 49 mg·g$^{-1}$ for acid-treated composites, respectively, from an initial concentration of 200 mg·ℓ$^{-1}$. At an initial $Pb^{2+}$ concentration of 100 mg·ℓ$^{-1}$, the heat-treated (in air) composite had an adsorption capacity of 80 mg·ℓ$^{-1}$. This is a significant increase from the 6 mg·g$^{-1}$ recorded with untreated EVA/C20A (Fig. 7).

The steep increase in the adsorption capacity during the early stages of the adsorption may be attributed to the abundance of adsorption sites available for binding. The increase in adsorption capacity with an increase in initial concentration can be attributed to the higher concentration of $Pb^{2+}$ ions vying for adsorption sites, resulting in a higher driving mass force. This effect can be attributed to adsorbate-adsorbent ratios at low initial concentrations which imply that metal ion adsorption involves higher energy sites (Naiya et al., 2009).

## Effect of adsorbent dose and temperature

The effect of adsorbent quantity and temperature on the adsorption of $Pb^{2+}$ on the composites heat-treated in air was investigated. Fig. 9 shows how the adsorption capacity changed with an increase in composite dose.

The adsorption capacity of $Pb^{2+}$ decreased as the dosage of the composite increased from 0.5 to 2.0 g·ℓ$^{-1}$. This may be attributed to the heavy metal ions competing for limited adsorption sites at lower composite dosage. At higher composite dosage, there would be more sites available for adsorption meaning that there would be not competition for by the $Pb^{2+}$ for active sites. A similar observation was reported by Zhi-rong et

http://dx.doi.org/10.4314/wsa.v38i4.6
Available on website http://www.wrc.org.za
ISSN 0378-4738 (Print) = Water SA Vol. 38 No. 4 July 2012
ISSN 1816-7950 (On-line) = Water SA Vol. 38 No. 4 July 2012

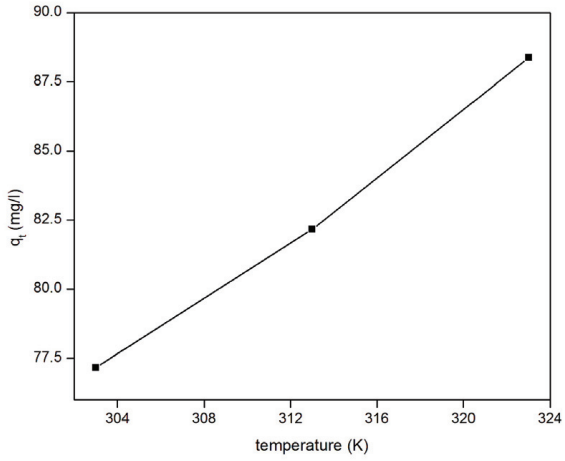


***Figure 10***
*Effect of temperature on the adsorption capacity of the heat-treated composite at an initial concentration of 100 mg·ℓ$^{-1}$ and pH 5.5*

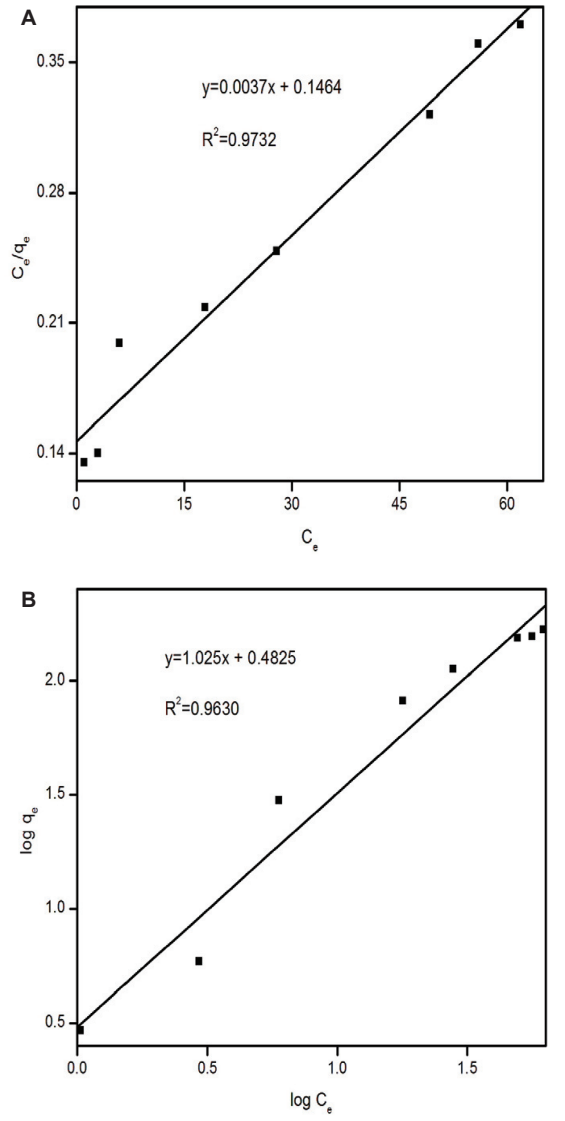


***Figure 11***
*Adsorption isotherms A: Langmuir; B: Freundlich isotherm*

al. (2010) on the removal of $Cu^{2+}$ and $Ni^{2+}$ using bentonite clay.

The results showing the effect of temperature on the extent of $Pb^{2+}$ adsorption onto the heat-treated composite are shown in Fig. 10. The temperatures used here are 303, 313 and 323 K.

The results indicate that in the temperature range used in this work the adsorption of $Pb^{2+}$ onto the composites increased with an increase in temperature. The observed increase in adsorption efficiency can be attributed to an increase in the movement of the ions with an increase in temperature as the density of the solution becomes lower. Adsorption is based on the collision between the adsorbate and the adsorbent.

## Adsorption isotherms

The Langmuir and Freundlich mathematical models were applied to define and analyse the adsorption isotherm and equilibrium properties of the adsorption of $Pb^{2+}$ onto the composites (Han et al., 2011). The equilibrium adsorption capacity ($q_e$) was calculated from the equilibrium concentration ($C_e$) using the following equation:

$$q_e = \frac{(C_o - C_e)v}{w_s} \quad (3)$$

The results are shown in Fig. 11. The correlation coefficients appear to suggest that both models may be suitable to describe the adsorption behaviour of $Pb^{2+}$ onto the composites under conditions used in this study.

The dimensionless constant $R_L$ was calculated from the Langmuir isotherm parameters and was found to be 0.1016. It has been widely reported that an $R_L$ value between 0 and 1 indicates favourable adsorption (Bello et al., 2010; Hosseini-Bandegharaei et al., 2011; Tofighy and Mohammadi, 2011). The constant, 1/*n* from the Freundlich isotherm is the heterogeneity coefficient and the heavy-metal removal is usually associated with chemical adsorption in cases where $n<1$. In this work, *n* was found to be 0.9757, suggesting a chemical interaction between $Pb^{2+}$ and the composite. Chemical binding was hypothesised considering the nucleophilic nature of the composite and the protic strength and electrophonic nature of the $Pb^{2+}$.

## Adsorption kinetics

The adsorption process occurs in at least 4 stages that can have different kinetic rates (Bystrzejewski et al., 2011). Firstly, the transport of the analyte will involve the migration of $Pb^{2+}$ from the bulk liquid to the composite particles. Since the composite particles would be enveloped by liquid film, the second stage of the adsorption process for $Pb^{2+}$ involves penetration through the film to gain contact with the composite particles. In the next step, there will be intraparticle diffusion of the $Pb^{2+}$ to reach the active sites of the composite. Lastly, adsorption will occur. It is imperative to identify the dominant (the slowest) step because it may control the kinetics of the adsorption process and therefore determine the removal rate of $Pb^{2+}$ from the aqueous solution.

However, since the adsorption experiments were done under vigorous shaking, the migration of the $Pb^{2+}$ from the liquid phase to the surface of the composite particles cannot be the rate-determining step. The interaction (binding) of $Pb^{2+}$ with the composite may not be the rate-limiting step because the adsorbate and adsorbent are hypothesised to bind instantly due to the opposite charges. Therefore, the rate-determining step could either be the migration of $Pb^{2+}$ through the ash pores (intraparticle diffusion) or the liquid-film-diffusion process. According to Alemayehua et al. (2011) the following equation,


http://dx.doi.org/10.4314/wsa.v38i4.6
Available on website http://www.wrc.org.za
ISSN 0378-4738 (Print) = Water SA Vol. 38 No. 4 July 2012
ISSN 1816-7950 (On-line) = Water SA Vol. 38 No. 4 July 2012

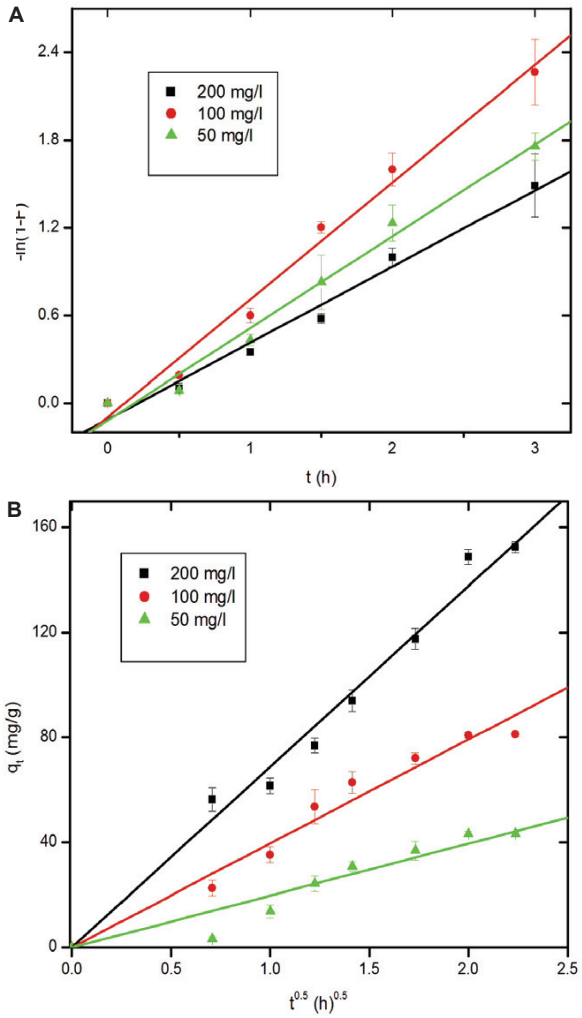


***Figure 12***
*Transport models for the removal of $Pb^{2+}$ with the heat-treated (in air) composite. A: liquid film diffusion; B: intraparticle diffusion*

known as the liquid-film model, can be applied to predict whether liquid-film diffusion is the rate-determining step in an adsorption process:

$$\ln(1-F) = -k_{fd}t \quad (4)$$

where:

$F$ is a constant ($F = q_t/q_e$)
$k_{fd}$ is the adsorption rate constant
$t$ is time (h)

A linear plot of $-ln(1-F)$ against $t$ passing through the origin (0,0) indicates that the liquid film diffusion is the rate-determining step of the kinetics of the adsorption process. According to Wang et al. (2011) and Li et al. (2011) the following equation can be applied to predict whether intraparticle diffusion is the rate-limiting step in an adsorption process:

$$q_t = K_p t^{1/2} + C \quad (5)$$

where:

$K_p$ is the intraparticle diffusion rate constant, in $mg \cdot g^{-1} \cdot h^{1/2}$

When the plot $q_t$ against $t^{1/2}$ is linear and passes through the origin (0, 0) then the intraparticle diffusion process is the primary limiting mechanism (Tofighy and Mohammadi, 2011). Figures 12A and 12B illustrate the results for liquid-film diffusion and intraparticle diffusion transport models, respectively.

Figure 12B shows that intraparticle diffusion was the rate-limiting stage. It is not surprising that intraparticle diffusion can be the primary rate-determining step in adsorption on the ash particle. The powder adsorbents may agglomerate significantly to larger particles when in contact with polar solvents like aquatic solutions of $Pb^{2+}$ (Bystrzejewski and Pyrzyn´Ska, 2011).

A study on adsorption kinetics does not rest only on the determination of the rate-limiting step, but also encompasses investigations of how different experimental conditions may influence the speed of an adsorption process, which can be understood by monitoring kinetic parameters. In the present work, batch adsorption kinetics of $Pb^{2+}$ with the composite particles derived from the EVA/C20A (in air) were investigated in terms of pseudo-first-order kinetics, pseudo-second-order kinetics, and as Natarajan, Khalaf and Elovich models. These models are described in the supporting information provided. The linear plots (shown in Fig. 13, next page) with good correlation coefficients (>0.900) imply that the adsorption of $Pb^{2+}$ under conditions used in this study conforms to the selected kinetic models.

Adsorption is expected to follow either pseudo-first-order or pseudo-second-order models. The correlation coefficients of the linear plots of these models may be used to predict the applicability of the models to fit the adsorption data. However, it is possible to obtain good correlation coefficients (>0.900) for both models as shown in the present work. Therefore, to identify the suitable model to describe the adsorption of the adsorbate onto the adsorbent, the kinetic constants ($k_i$, $i$=1 or 2) and, more importantly, the calculated equilibrium adsorption capacity ($q_{e,cal}$) are compared. The $k_1$, $k_2$ and $q_{e,cal}$ for the adsorption of $Pb^{2+}$ onto the ash were calculated and are given in Table 2. The results show lower kinetic constant values for the pseudo-first-order model compared to the pseudo-second-order model. The $q_{e,cal}$ values for the pseudo-second-order model were closer to the experimental values (mean $q_{e,exp}$) when compared to those of the pseudo-first-order model at the initial concentrations studied.

The validity of the pseudo first-order model and pseudo second-order model was tested by a normalised standard deviation, $\Delta q$ (%), which was calculated using the following equation (Hosseini-Bandegharaei, 2011):

**Table 2**
**Summarised kinetic constants**

| $C_o$ (mg·ℓ⁻¹) | Mean $q_{e,exp}$ | Pseudo-first-order | | Pseudo-second-order | | Elovich | | N&K[a] |
|---|---|---|---|---|---|---|---|---|
| | | $q_{e,cal}$ | $k_1$ | $q_{e,cal}$ | $k_2$ x10⁻³ | $\alpha$ | $B$ | $K_N$ |
| 200 | 152.3 | 90.02 | 1.177 | 192.3 | 5.556 | 142.2 | 0.0159 | 0.3399 |
| 100 | 81.69 | 54.60 | 1.748 | 115.1 | 3.025 | 100.6 | 0.0301 | 0.4242 |
| 50 | 43.08 | 24.53 | 1.620 | 61.94 | 4.102 | 43.10 | 0.0511 | 0.5122 |

[a]*Natarajan and Khalaf*

http://dx.doi.org/10.4314/wsa.v38i4.6
Available on website http://www.wrc.org.za
ISSN 0378-4738 (Print) = Water SA Vol. 38 No. 4 July 2012
ISSN 1816-7950 (On-line) = Water SA Vol. 38 No. 4 July 2012

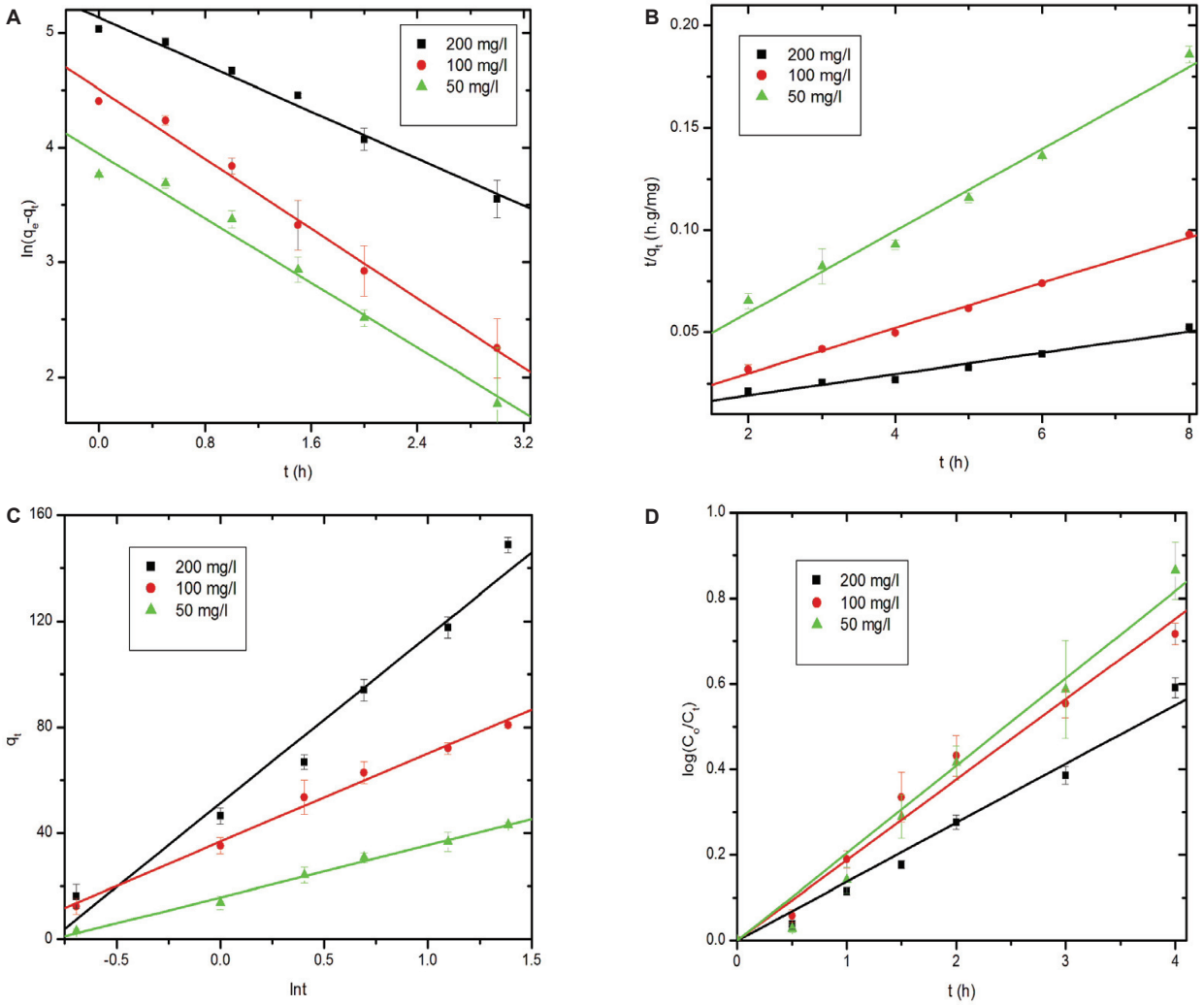


***Figure 13***
*Kinetic modelling for the adsorption of $Pb^{2+}$ onto the heat-treated (in air) composite. A: pseudo-first-order; B: pseudo-second-order; C: Elovich; D: Natarajan and Khalaf*

$$\Delta q(\%) = 100\sqrt{\frac{\sum\left[\left(q_{e,exp} - q_{e,cal}\right)/q_{e,exp}\right]^2}{N-1}} \qquad (6)$$

where:

$q_{e,exp}$ and $q_{e,cal}$ are experimental and calculated amounts of $Pb^{2+}$ adsorbed onto the composites at time *t; N* is the number of measurements made.

It was established that the pseudo-second-order model gave better standard deviations than the pseudo-first-order model. The calculated values from the pseudo-first-order model were found to be 29.72%, 25.66% and 32.23%, corresponding to 200 mg·ℓ$^{-1}$, 100 mg·ℓ$^{-1}$ and 50 mg·ℓ$^{-1}$, respectively. On the other hand, the normalised standard deviations calculated from the pseudo-second-order model were as follows: 16.85% (200 mg·ℓ$^{-1}$), 24.27% (100 mg·ℓ$^{-1}$) and 26.44% (50 mg·ℓ$^{-1}$). These values confirm that the adsorption of $Pb^{2+}$ onto the heat-treated (in air) composites may best be described by pseudo-second-order kinetics.

The results presented in Table 2 show that reliable conclusions can be drawn from the Elovich parameters. The higher values of α compared to $\beta$ indicate that there was more adsorption than desorption during the experiment. This confirms that the adsorption of $Pb^{2+}$ was through chemical adsorption. It is widely accepted that chemical adsorption is an irreversible process. It can be deduced from α values that $Pb^{2+}$ removal is faster at the higher initial concentrations during the early stages of adsorption. This observation can be explained by the fact that there are more $Pb^{2+}$ competing for the active sites in the composites. This was further confirmed by the Natarajan and Khalaf model kinetic constants ($K_N$), which are seen to increase with a decrease in initial concentration.

The effectiveness of the composites in removing heavy metals from water, especially in terms of adsorption capacity, can be shown by comparing the experimental values obtained with a few values for sorption capacities reported in the literature, as shown in Table 3. The sorbents summarised in Table 3 have been described as good adsorbents elsewhere. The heat-treated composites showed superior adsorption capabilities compared to EVA/C20A and acid-treated EVA/C20A composites.

## Conclusion

The results presented in this study demonstrate that the non-biodegradable and hydrophobic EVA/C20A composites could


http://dx.doi.org/10.4314/wsa.v38i4.6
Available on website http://www.wrc.org.za
ISSN 0378-4738 (Print) = Water SA Vol. 38 No. 4 July 2012
ISSN 1816-7950 (On-line) = Water SA Vol. 38 No. 4 July 2012

| Table 3<br>Sorption capacity of different powder sorbents | | |
|---|---|---|
| **Source of adsorbent** | **Sorption capacity ($mg \cdot g^{-1}$)** | **Reference** |
| Sugarcane bagasse | 38 | Mohan et al., 2002 |
| EVA/C20A composite (acidified) | 49 | Current study |
| Scrap rubber | 100 | McKay et al., 1998 |
| EVA/C20A composite (in air) | 153 | Current study |
| Fly ash | 198 | Apak et al., 1998 |

be suitable heavy-metal adsorbents after acid- and heat-treatments. With an adsorption capacity of 153 $mg \cdot g^{-1}$, the heat-treated composite was found to be more effective in the removal of $Pb^{2+}$ from an initial concentration of 200 $mg \cdot \ell^{-1}$, when compared to 49 $mg \cdot g^{-1}$ observed for the acid-treated composite. The adsorption data for heat-treated composites were fitted to isotherm and kinetic models. Equilibrium isotherms and Elovich models revealed that the removal of $Pb^{2+}$ was mostly a result of chemisorption.

## Acknowledgements

This study was funded by the National Research Foundation (NRF) and the University of Johannesburg (UJ).

## References

ALEMAYEHUA E, THIELE-BRUHNB S and LENNARTZA B (2011) Adsorption behaviour of Cr(VI) onto macro- and micro-vesicular volcanic rocks from water. *Sep. Purif. Technol*. **78** (1) 55–61.

AL-ATTAR AM (2011) Antioxidant effect of vitamin E treatment on some heavy metals-induced renal and testicular injuries in male mice. *Saudi J. Biol. Sci*. **18** (1) 63–72.

APAK RE, HUGUL M and HIZAL J (1998) Heavy metal cation retention by unconventional sorbents (red muds and fly ashes). *Water Res*. **32** (2) 430–440.

BAHRAMIAN AR, KOKABI M, FAMILI MHN and BEHESHTY MH (2008) High temperature ablation of kaolinite layered silicate/phenolic resin/asbestos cloth nanocomposite. *J. Hazard. Mater.* **150** (1) 136–145.

BAI J, XIAO R, CUI B, ZHANG K, WANG X, LIU Q, GAO H and HUANG L (2011) Assessment of heavy metal pollution in wetland soils from the young and old reclaimed regions in the Pearl River Estuary, South China. *Environ. Pollut*. **159** (3) 817–824.

BELLO OS, ADELAIDE OM, ABDUL HAMMED M and ABDUL MUIZ POPOOLA O (2010) Kinetic and equilibrium studies of methylene blue removal from aqueous solution by adsorption on treated sawdust. *Macedonian J. Chem. Chem. Eng.* **29** (1) 77–85.

BESSADOK A, MARAIS S, GOUANVE´ F, COLASSE L, ZIMMERLIN I, ROUDESLI S and ME´TAYER M (2007) Effect of chemical treatments of Alfa (*Stipa tenacissima*) fibres on water-sorption properties. *Comp. Sci. Technol*. **67** (3–4) 685–697.

BYSTRZEJEWSKI M and PYRZYN´SKA K (2011) Kinetics of copper ions sorption onto activated carbon, carbon nanotubes and carbon-encapsulated magnetic nanoparticles. *Coll. Surf. A: Physicochem. Eng. Aspects* **377** (1–3) 402–408.

DLAMINI DS, MISHRA SB, MISHRA AK and MAMBA BB (2011a) Ethylene vinyl acetate and polycaprolactone–organoclay nanocomposite: thermal, mechanical and morphological properties. *J. Inorg. Organomet. Polym*. **21** (2) 229–236.

DLAMINI DS, MISHRA SB, MISHRA AK and MAMBA BB (2011b) Comparative studies of the morphological and thermal properties of clay/polymer nanocomposites synthesized via melt blending and modified solution blending methods. *J. Comp. Mater.* **45** (21) 2211–2216.

HAN J, DAI J and GUO R (2011) Highly efficient adsorbents of poly(o-phenylenediamine) solid and hollow sub-microspheres towards lead ions: A comparative study. *J. Colloid Interface. Sci.* **356** (2) 749–756.

HULL TR, PRICE D LIU Y WILLS CL and BRADY J (2003) An investigation into the decomposition and burning behaviour of EVA nanocomposite materials. *J. Polym. Deg. Stab.* **82** (1) 365–371.

HOSSEINI-BANDEGHARAEI A, HOSSEINI MS, JALALABADI Y, SARWGHADI M, NEDAIE M, AHERIAN A, GHAZNAVI A and EFTEKHARI A (2011) Removal of Hg(II) from aqueous solutions using a novel impregnated resin containing 1-(2-thiazolylazo)-2-naphthol (TAN). *Chem. Eng. J.* **168** (3) 1163–1173.

KILIARIS P and PAPASPYRIDES CD (2010) Polymer/layered silicate (clay) nanocomposites: An overview of flame retardancy. *Prog. Polym. Sci*. **35** (7) 902–958.

KOYUNCU H (2008) Adsorption kinetics of 3-hydroxybenzaldehyde on native and activated bentonite. *Appl. Clay Sci*. **38** (3–4) 279–287.

LI L, LIU F, JING X, LING P and LI A (2011) Displacement mechanism of binary competitive adsorption for aqueous divalent metal ions onto a novel IDA-chelating resin: Isotherm and kinetic modelling. *Water Res*. **45** (3) 1177–1188.

LIUA M, LIUA X, DINGB W and WUA L (2011) Monitoring stress levels on rice with heavy metal pollution from hyperspectral reflectance data using wavelet-fractal analysis, *Intern. J. Appl. Earth Obs. Geoinf.* **13** (2) 246–255.

LONGA Y-Y, SHENA D-S, WANGB H-T, LUB W-J and ZHAOB Y (2011) Heavy metal source analysis in municipal solid waste (MSW): Case study on Cu and Zn. *J. Hazard. Mater.* **186** (2–3) 1082–1087.

McKAY G, VONG B and PORTER JF (1998) Isotherm studies for the sorption of metal ions onto peat. *Adsorp. Sci. Technol*. **16** (1) 51–66.

MOHAN D and SINGH KP (2002) Single- and multi-component adsorption of cadmium and zinc using activated carbon derived from bagasse - an agricultural waste, *Water Res*. **36** (9) 2304–2318.

NAIYA TK, BHATTACHARYA AK and DAS SK (2009) Adsorption of Cd(II) and Pb(II) from aqueous solutions on activated alumina. *J. Coll. Inter. Sci*. **333** (1) 14–26.

PERIASAMY K and NAMASIVAYAM C (1996) Removal of copper(11) by adsorption onto peanut hull carbon from water and copper plating industry wastewater. *Chemosphere* **32** (4) 769–789.

TOFIGHY MA and MOHAMMADI T (2011) Adsorption of divalent heavy metal ions from water using carbon nanotube sheets. *J. Hazard. Mater.* **185** (1)140–147.

TONGPOOTHORN W, SRIUTTHA M, HOMCHAN P, CHANTHAI S and RUANGVIRIYACHAI C (2011) Preparation of activated carbon derived from *Jatropha curcas* fruit shell by simple thermo-chemical activation and characterization of their physico-chemical properties. *Chem. Eng. Res. Des.* **89** (3) 335–340.

VARGAS AMM, CAZETTA AL, GARCIA CA, MORAES JCG, NOGAMI EM, LENZI E, COSTA WF and ALMEIDA VC (2011) Preparation and characterization of activated carbon from a new raw lignocellulosic material: Flamboyant (*Delonix regia*) pods. *J. Environ. Manage.* **92** (1) 178–184.

WANG XS, LU ZP, MIAO HH, HE W and SHEN HL (2011) Kinetics of Pb (II) adsorption on black carbon derived from wheat residue. *Chem. Eng. J.* **166** (3) 986–993.

WEI Y-T, ZHENG Y-M and CHEN JP (2011) Enhanced adsorption of arsenate onto a natural polymer-based sorbent by surface atom transfer radical polymerization. *J. Colloid Interface Sci.* **356** (1) 234–239.

ZHI-RONG L and SHAO-QI Z (2010) Adsorption of copper and nickel on Na-bentonite. *Proc. Saf. Environ. Prot.* **88** 62–66.

# Appendix 1: Data treatment

## Adsorption isotherms

**Langmuir isotherm:** A linear form of the Langmuir isotherm was given by the following equation:

$$\frac{C_e}{q_e} = \frac{1}{bQ_o} + \frac{C_e}{Q_o} \quad (1)$$

The constant $Q_o$ signified the adsorption capacity (mg·g$^{-1}$) and $b$ is related to the energy of adsorption (ℓ·mg$^{-1}$). If the data fits a Langmuir isotherm a plot of $C_e/q_e$ vs. $C_e$ should give a linear plot. Energy of adsorption ($b$) and the initial concentration ($C_o$) are related to the constant $R_L$ as follows:

$$R_L = \frac{1}{1 + bC_o} \quad (2)$$

**Freundlich isotherm:** The well-known logarithmic form of the Freundlich model is given by the following equation:

$$\log q_e = \log K_F + \frac{1}{n}\log C_e \quad (3)$$

where:

$q_e$ is the amount adsorbed at equilibrium (mg·g$^{-1}$)
$C_e$ is the equilibrium concentration of the adsorbate
$K_F$ and $n$ are the Freundlich constants

## Kinetic models

**The pseudo-first-order model** (this equation is also called the Lagergren equation):

$$\frac{dq_t}{dt} = k_1(q_e - q_t) \quad (4)$$

where:

$q_e$ and $q_t$ refer to the amounts of $Pb^{2+}$ (mg·ℓ$^{-1}$) adsorbed on the composites at equilibrium time and time $t$ (h) and $k_1$ as the Lagergren rate constant (min$^{-1}$), respectively.

Integrating the above equation with the boundary conditions, $t = 0$ to $t = t$ and from $q_t = 0$ to $q_t = q$ gives a linear version of Eq. (4):

$$\log(q_e - q_t) = \log(q_e) - \frac{k_1}{2.303}t \quad (5)$$

The kinetic parameter $k_1$, and the amount absorbed at equilibrium can be experimentally determined from the plot of log ($q_e$-$q_t$) vs. $t$ which gives a linear graph where the y-intercept is log ($q_e$) and $k_1$ is calculated from the slope. The results are shown in Fig. 13A.

**The pseudo-second-order model:** The pseudo-second-order equation is expressed as Eq. (6) and the linear form is shown in Eq. (7).

$$\frac{dq_t}{dt} = k_2(q_e - q_t)^2 \quad (6)$$

$$\frac{t}{q_t} = \frac{1}{k_2 q_e^2} + \frac{t}{q_e} \quad (7)$$

where:

$k_2$ is the second-order rate constant. If the second-order kinetics is applicable, the plot of $t/q_t$ against t should show a linear relationship.

**The Elovich model:** The Elovich model equation is generally expressed as:

$$q_t = \frac{1}{\beta}\ln(\alpha\beta) + \frac{1}{\beta}\ln(t) \quad (8)$$

where:

α is the initial adsorption rate (mg·g$^{-1}$·min), and β is the desorption constant (g·mg$^{-1}$) during any one experiment.

If $Pb^{2+}$ adsorption fits the Elovich model, a plot of $q_t$ vs. l$n$ ($t$) should yield a linear relationship with a slope of $\beta^{-1}$ and an intercept of $\beta^{-1}$ ln (αβ).

**Natarajan and Khalaf model:** This model was used to develop a relation between the initial concentration and the concentration at any time $t$. The Natarajan and Khalaf equation is expressed as follows:

$$\log \frac{C_o}{C_t} = \frac{K_N}{2.303} t \quad (9)$$

where:

$K_N$ is a constant obtained from the slope of log ($C_o/C_t$) vs. $t$



http://dx.doi.org/10.4314/wsa.v38i4.6
Available on website http://www.wrc.org.za
ISSN 0378-4738 (Print) = Water SA Vol. 38 No. 4 July 2012
ISSN 1816-7950 (On-line) = Water SA Vol. 38 No. 4 July 2012